Chiang Mai J. Sci. 2021; 48(5) : 1430-1443
http://epg.science.cmu.ac.th/ejournal/
Contributed Paper

The Numerical Visualization of Air Pollution Propagation from a Single Generator to an Observed Area

Udomsak Rakwongwan*[a], Arnon Archankul [b], Sanae Rujivan [b,c] and Perter Bastian [d]

[a] Department of Mathematics, Faculty of Science, Kasetsart University, Bangkok 10900, Thailand
[b] Division of Mathematics and Statistic, School of Science, Walailak University, Nakhon Si Thammarat 80161, Thailand
[c] Center of Excellence in Data Science for Health Study, Walailak University, Nakhon Si Thammarat 80161, Thailand
[d] Interdisciplinary Center for Scientific Computing, Heidelberg University, Heidelberg D-69120, Germany

*Author for correspondence; e-mail: udomsak.ra@ku.th

Received: 8 September 2020
Revised: 18 February 2021
Accepted: 14 May 2021

Abstract

This paper studies the propagation of the air pollutants released from a single generator such as an industrial chimney to an observed area such as a residential area or an agricultural land in two dimensions. The aims are to develop a model to visualize the propagation of the pollutants over time and to compute an average concentration of the pollutants on the observed area subject to various factors such as wind speed, the distance from the observed area to the generator, and how the pollutants are emitted. We model the problem as a system of partial differential equations composed of the Navier-Stokes and the advection-diffusion equations and numerically solve it by the finite element method. To illustrate the technique, we visualized the propagation of the pollutants for several emission case studies and computed their concentrations on an observed area over time.

Keywords: air pollution management, advection-diffusion equation, Navier-Stokes equations, finite element method

1. Introduction

Air pollution has been one of the main causes to both acute and chronic health issues. In 2012, according to World Health Organization [1], there were around 7 million people who lost their lives due to air pollution exposure. An estimate of 9 out of 10 people are exposed to air pollution which exceeds the safe level recommended by WHO. In addition, many studies have shown that air pollution has several negative effects on agricultural production. It may leave markings on crop leaves, reduce production yield, or result in premature death. The pollutants also greatly affect flowering and fruiting [2]. The effects of Sulphur Dioxide, Fluorides, wet deposited acidity, and pollutants mixtures were detailed in [3]. Roughly around 36-50 % relative yield losses for wheat are from long-lived greenhouse gases (LLGHGs) and short-lived climate pollutants (SLCPs), see [4]. Thus, a systematic measure for air pollution management is crucially important and urgently needed.

There have been several works dealing with air pollution management. [5] studied the effects of the wind direction which was described by Navier-Stokes equations on the propagation of the pollutants in the air. Boussinesq approximation was also integrated to Navier-Stokes equations to take into account the Buoyant force exerting from the temperature change within the observed domain. One of the most popular tools used in the study of the diffusion of the air pollution in the literature is the finite element method (FEM); see e.g. [6]. [7] considered the propagation of the pollutants emitted from a single generator by comparing the simulations of air pollution diffusion obtained from FEM and finite difference method (FDM) and concluded that both methods were efficient and suitable for air pollution emission control. In addition to [7], in a two-dimensional space, the time dependent behavior of the air pollution was studied in [8] with an inversion layer by utilizing the fractional step method. While similarly in [9], the pollutants emitting from a single generator were studied under different atmosphere conditions using explicit FDM and Lazarus programming software. In addition to the studies of the air pollutants emitted from a single generator, [10] considered a smoke dispersion problem with two sources with a structural obstacle. The propagation of the pollutants from multiple sources above an industrial area to a residential area was studied in [11]. The distribution of the pollutants on a larger domain was studied by [12] and [13]. The first one studied the propagation of the pollutants in an urban area flowing through obstacles, while the latter studied that on a regional scale.

This paper studies the propagation of the industrial air pollution emitted from industrial activities such as the burning of fossil fuels in electricity generation, which is one of the major sources of air pollution, to an observed domain such as a residential area or an agricultural land for different emission cases. We first propose a mathematical model for the air pollution propagation and numerically solve it using the finite element method for several cases namely “steady emission”, “periodic emission” and “discontinuous emission” depending on how the pollution is emitted. The average concentration of the pollutants over time on the observed area for each case is also computed. Although this work is based on many assumptions which might not be valid in real-world problems, it can still be useful for regulators as well as for factories to estimate the air pollution level.

The paper is organized as follows. Section 2 describes the mathematical model used to tackle the problem, the emission cases, as well as the method and the packages used to numerically solve the model. Section 3 shows the results which are the visualization of the air pollutant propagation and the average concentration of the pollutants on the observed area over time for each emission case. Section 4 is the conclusion.

2. Materials and Methods

2.1 Materials

2.1.1 The model

We study the effects of the air pollution emitted from a single source such as an industrial factory on an observed area. The domain of the problem is denoted by Ω while Ω_0 denotes the observed area (see Figure 1). Γ_i for $i = 1, 2, ..., 8$ denote the boundaries of the problem. Γ_4 is the air pollution generator.

This problem can be viewed as a fluid dynamic problem which can be mathematically described by the following system of partial differential equations.

$$\frac{\partial \mathbf{u}}{\partial t} + (\mathbf{u} \cdot \nabla)\mathbf{u} = -\frac{1}{\rho}\nabla p + \nu\Delta\mathbf{u} + (1 - \beta(\theta - \theta_0))\mathbf{g} \tag{0.1}$$

$$\nabla \cdot \mathbf{u} = 0 \tag{0.2}$$

$$\frac{\partial \theta}{\partial t} + (\mathbf{u} \cdot \nabla)\theta = \kappa\Delta\theta \tag{0.3}$$

$$\frac{\partial C}{\partial t} + (\mathbf{u} \cdot \nabla)C = (\nabla \cdot \mathbf{K}\nabla)C \tag{0.4}$$

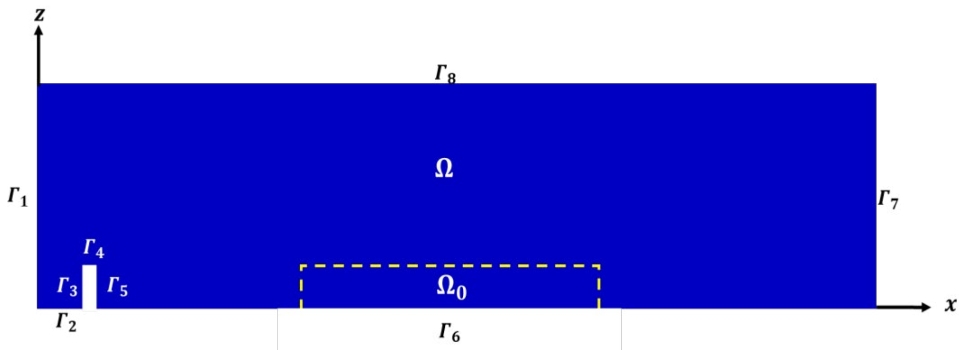

Figure 1. The problem domain Ω, the observed area Ω_1 and the boundaries Γ_i.

where $\mathbf{u} = [u \quad w]^T$, $\mathbf{g} = [0 \quad g]^T$, and $\mathbf{K} = \begin{pmatrix} K_x & 0 \\ 0 & K_z \end{pmatrix}$.

$u = u(x,z,t)$ is the velocity of the fluid along the x axis at the position $(x,z) \in \Omega$ and time $[m/s]$,

$w = w(x,z,t)$ is the velocity of the fluid along the z axis at the position $(x,z) \in \Omega$ and time $[m/s]$,

$p = p(x,z,t)$ is the pressure of the fluid at the position $(x,z) \in \Omega$ and time t $[kg/ms^2]$,

$\theta = \theta(x,z,t)$ is the temperature of the fluid at the position $(x,z) \in \Omega$ and time t $[K]$,

$C = C(x,z,t)$ is the concentration of the pollutants at the position $(x,z) \in \Omega$ and time t $[\mu g/m^2]$,

$K_x = K_x(x,z,t)$ is the diffusion coefficient of the pollutants along the x axis at the position $(x,z) \in \Omega$ and time t $[m^2/s]$,

$K_z = K_z(x,z,t)$ is the diffusion coefficient of the pollutants along the z axis at the position $(x,z) \in \Omega$ and time t $[m^2/s]$,

ρ is the density of the air $[kg/m^3]$,

ν is the kinematic viscosity of the air $[m^2/s]$,

β is the thermal expansion coefficient $[K^{-1}]$,

θ_0 is the temperature of the fluid at the reference point $[K]$,

g is the acceleration due to gravity $[m/s^2]$, and

κ is the thermal diffusivity $[m^2/s]$.

Equations (1.1)-(1.3) are Navier-Stokes equations, derived from the laws of conservation of mass, momentum and energy, which describe the flow of incompressible fluids; see e.g. [14] and [15]. Equation (1.4) is called an advection-diffusion equation; see e.g. [16], which describes the propagation of the pollutants in the air.

2.1.2 Initial conditions and boundary conditions

To solve the system of the partial differential equations (1.1)-(1.4), the initial conditions and the boundary conditions are needed to be specified. The initial conditions are as follows:

$u(x,z,0) = u_0(x,z)$ is the initial wind velocity along the x axis at the position $(x,z) \in \Omega$ at time $t = 0$,

$w(x,z,0) = w_0(x,z)$ is the initial wind velocity along the z axis at the position $(x,z) \in \Omega$ at time $t = 0$,

$\theta(x,z,0) = \theta_0(x,z)$ is the initial temperature at the position $(x,z) \in \Omega$ at time $t = 0$,

$C(x,z,0) = C_0(x,z)$ is the initial pollutants concentration at the position $(x,z) \in \Omega$ at time $t = 0$.

All of the eight boundaries, $\Gamma_1 - \Gamma_8$, in the model as seen in Figure 1 are specified as follows:

Γ_1 $\quad u(x,z,t) = u_1(x,z,t)$, $\quad w(x,z,t) = 0$,
$\theta(x,z,t) = \theta_1(x,z,t)$, $\quad C(x,z,t) = 0$,

$\Gamma_{2,3,5,6,8}$ $\quad u(x,z,0) = 0$, $\quad w(x,z,t) = 0$,

$$\frac{\partial \theta(x,z,t)}{\partial z} = 0, \qquad \frac{\partial C(x,z,t)}{\partial z} = 0,$$

Γ_4 $\quad u(x,z,0) = 0$, $\quad w(x,z,t) = w_4(x,z,t)$,
$\theta(x,z,t) = \theta_4(x,z,t)$,
$C(x,z,t) = C_4(x,z,t)$,

Γ_7
$$\nu \frac{\partial u(x,z,t)}{\partial x} = \frac{1}{\rho} p(x,z,t),$$
$$\nu \frac{\partial w(x,z,t)}{\partial x} = 0,$$
$$\theta(x,z,t) = 0, \qquad C(x,z,t) = 0,$$

where, $u_1(x,z,t)$ is the wind velocity along the x axis at the position (x,z) on the boundary Γ_1 and time $t > 0$,

$\theta_1(x,z,t)$ is the temperature along at the position (x,z) on the boundary Γ_1 and time $t > 0$,

$w_4(x,z,t)$ is the wind velocity along the z axis at the position (x,z) on the boundary Γ_4 and time $t > 0$,

$\theta_4(x,z,t)$ is the temperature along at the position (x,z) on the boundary Γ_4 and time $t > 0$,

$C_4(x,z,t)$ is pollutants concentration at the position (x,z) on the boundary Γ_4 and time $t > 0$.

It can be seen that the wind speed along the x axis on the boundary Γ_4 is always zero, while the wind speed along the z axis is $w_4(x,t)$, which is a function of x and t. This is because Γ_4 is the pollutant generator such as a tall industrial factory chimney. There might be some wind blowing out at the top of the chimney along with the pollutants $\theta_4(x,t)$ refers to the temperature at the top of the tower. $C_4(x,t)$, which is a function of x and t, describes the concentration of the pollutants at each point x over time t. In other words, it determines how the pollutants are emitted. The outflow boundary Γ_7 is described by the improved "do nothing" condition by [17] which could remove the unphysical eddies in the lower right corner of the concentration plots.

2.1.3 Case study

In this subsection, we describe the emission cases namely "steady emission", "periodic emission" and "discontinuous emission" which can be determined by the concentration of the pollutants emitted from the generator over time $C_4(x,t)$.

(a) Steady emission

This is the case when the pollutants are emitted continuously with a constant concentration. In other words,

$$C_4(x,t) = c_s,$$

for all $t > 0$ and c_s is a constant.

(b) Periodic emission

For periodic emission, the concentration of the pollutants at the boundary Γ_4 over time can be expressed in terms of a periodic function as

$$C_4(x,t) = \frac{c_p}{2}(1 - \cos(\frac{\pi t}{t_p})),$$

for all $t > 0$. c_p is the maximum concentration of the pollutants emitted from the generator, and t_p is the time when the concentration c_p is emitted.

(c) Discontinuous emission

The concentration of pollutants released from the source, for discontinuous emission case, is a constant c_d at $t = t_d, 2t_d, 3t_d, \ldots$ and zero otherwise. In other words,

$$C_4(x,t)=\begin{cases} c_d, & t=t_d k \text{ for } k\in\mathbb{N}_0 \\ 0, & \text{otherwise} \end{cases},$$

for all $t>0$.

2.2 Methods

2.2.1 Numerical method

It is difficult to solve the system of the partial differential equations (1.1)-(1.4) analytically given the initial and the boundary conditions. There are several numerical techniques commonly used in order to solve the problem such as the finite difference method, the finite element method, and the finite volume method. In this paper, the finite element method is employed.

One of the advantages of using the finite element method is that the domain does not need to be discretized equally in size. We can finely discretize the focused area into smaller pieces. This reduces the computational time greatly. For this problem, our domain is discretized as in Figure 2. The discretized domain is generated with Gmsh, a finite-element mesh generator developed by [18].

In this paper, we use a software called "the distributed and unified numeric environment" or DUNE which is a software for solving systems of partial differential equations using the finite element method; see e.g. [19] and [20].

2.2.2 Average concentration of the pollutants on the observed area

In addition to visualizing the propagation of the pollutants on the domain Ω, we are interested in the average concentration of the pollutants on the observed area Ω_0 which indicates how severely the observed area is affected by the air pollution.

As our domain is not equally discretized (see Figure 2), the computation of the average concentration of the air pollutants over the observed area is not straightforward. One of the methods is to equally discretize the observed domain into $(m-1)\times(n-1)$ smaller rectangles and compute the mean of the average concentration in the rectangles (see Figure 3). Mathematically, the average of pollutant concentration on the observed area as a function of time, $\bar{C}(t)$, can be approximated by

$$\bar{C}(t)=\frac{\iint_{(x,z)\in\Omega_0} C(x,z,t)\,dxdz}{\|\Omega_0\|}\approx\frac{\sum_{i=1}^{m-1}\sum_{j=1}^{n-1} C_{ij}\Delta x\Delta z}{\|\Omega_0\|}$$

where Ω_0 is discretized into $(m-1)\times(n-1)$ rectangles as shown in Figure 3,

$\|\Omega_0\|$ is the area of Ω_0 which is equal to $l\times h$,

$\Delta x, \Delta z$ are the lengths of the rectangles which equal $\frac{l}{m}$ and $\frac{h}{n}$ respectively,

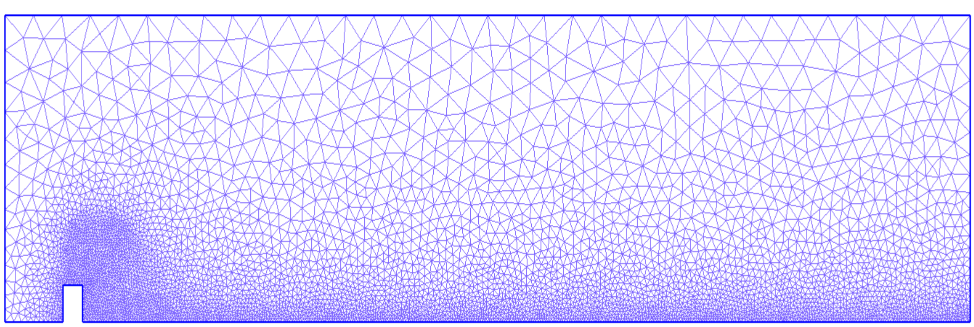

Figure 2. The discretized problem domain for the finite element method.

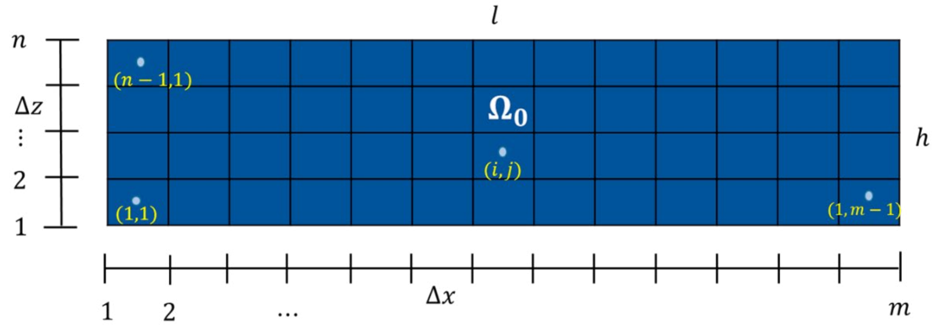

Figure 3. The observed domain Ω_0 which is discretized into $(m-1)\times(n-1)$.

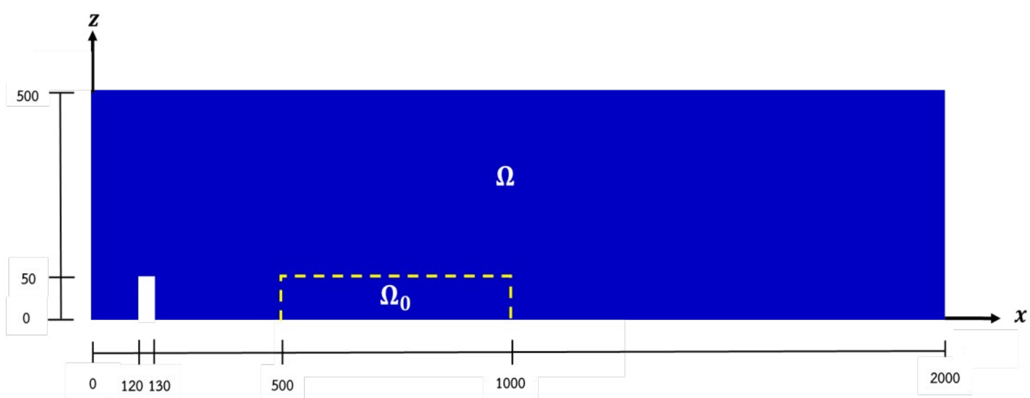

Figure 4. The problem domain Ω and the observed area Ω_0 with the specified heights and widths.

C_{ij} is an average of the concentration $C(x,z,t)$ over the rectangle (i,j).

3. Results and Discussion

To illustrate the application of the model to a real-world problem, we consider a two-dimensional domain with the height of 500 meters and the width of 2000 meters; see Figure 4. The height and the width of the observed area are 50 meters and 500 meters respectively. The pollutant generator is 10 meters wide and 50 meters tall. The distance between the center of the generator to the observed area is 370 meters.

3.1 The Parameters

To numerically compute the solutions, the parameters, the initial conditions and the boundary conditions mentioned in Sections 2.1-2.2 are needed to be first specified. The parameters are subject to the property of the fluid under some certain assumptions. Unless otherwise stated, the parameter values used in the computation are as in Table 1. The parameters are the standard values at 300 Kelvin; see [21].

In this paper, we assume that the effect of the wind on the pollutant propagation along the x axis is overwhelmingly higher than that from the diffusion. In other words, $u\frac{\partial C}{\partial x} >> \frac{\partial}{\partial x}K_x\frac{\partial C}{\partial x}$.

Table 1. The parameter values used in the computation.

Parameter	Value
Air density (ρ)	$1.18\ [kg/m^3]$
Kinematic viscosity of the air (ν)	$1.57\times10^{-5}\ [m^2/s]$
Thermal expansion coefficient (β)	$1.75\times10^{-3}\ [K^{-1}]$
Temperature of the fluid at the reference point (θ_0)	$400\ [K]$
Acceleration due to gravity (g)	$9.8\ [m/s^2]$
Thermal diffusivity (κ)	$2.2\times10^{-5}\ [m^2/s]$

Thus, the value of the diffusion coefficient along the x axis, K_x, is assumed to be zero.

The diffusion coefficient along the z axis is usually a function depending on atmospheric stability which can be classified into 3 classes namely a stable condition, an unstable condition, and a neutral condition. In this computation, we only consider the neutral condition case whose vertical diffusion coefficient, from [22], can be written as

$$K_z = K_z(z) = 0.4u_*ze^{-\frac{z}{H}}$$

where a fractional velocity u_* and an average height H of the surface at the bottom of the domain which is assumed to be flat and smooth are 0.16 $[m/s]$ and 1×10^{-5} $[m]$ respectively.

The initial velocities along the x axis and z axis for the neutral condition case are given as follows,

$$u(x,z,0) = u_0\left(\frac{z}{z_0}\right)^{0.15},$$

$$w(x,z,0) = 0$$

where u_0 is the velocity along the x axis at the height of z_0. Throughout this computation, $u_0 = 4.4\ [m/s]$ and $z_0 = 100\ [m]$.

For the initial air temperature, we assume that the air is dry and there is no propagation of the energy to the environment. The temperature drops one degree Celsius for each 100 meters from the ground. This is called adiabatic process. The initial temperature can then be expressed as

$$\theta(x,z,0) = -0.01z + 300.$$

On the boundary Γ_1, $u_1(x,z,t) = u(x,z,0)$ and $\theta_4(x,z,t) = \theta(x,z,0)$while on the boundary Γ_4, $w_4(x,z,t) = 14$, $\theta_4(x,z,t) = 400$, and $C_4(x,t)$ is dependent on each study case. In other words, we assume that the wind blows out of the top of the chimney at the constant speed of 14 $[m/s]$, and the temperature at the top of the chimney is 400 $[K]$.

3.2 The Results

In this subsection, we visualize the propagation of the pollutants by plotting the concentration of the pollutants on the domain Ω over time as well as compute an average of the pollutant concentration, $\overline{C}(t)$, on the observed area Ω_0 for each emission case mentioned in Section 2.1.3.

3.2.1 Steady emission

We first consider the case where the pollutants are emitted steadily with the concentration of 1 $[g/m^2]$. In other words,

$$C_4(x,t) = 1$$

for all $t > 0$.

Figure 5 shows the propagation of the pollutants after 6.72, 44.24, and 165.20 seconds. It can be seen that the pollutants are propagated in the wind direction and diffused along the z axis. We can also see the circulation of the pollutants the over time.

Figure 6 shows the average concentration of the pollutants in the observed area Ω_0 as a function of time. We see that the observed area starts to suffer from the air pollution after 7 seconds. Then the average concentration of the pollutants rises steeply until around 42 seconds when it starts to increase steadily. In other words, if the pollutants are emitted steadily, the concentration of the pollution will initially rise drastically and continue to increase steadily after some point in time.

3.2.2 Periodic emission

We consider the case where the pollutants are emitted periodically with the maximum concentration c_p of 1 $[g/m^2]$ and the period of 1.4 seconds, or

$$C_4(x,t) = \frac{1}{2}(1 - \cos(\frac{\pi t}{1.4}))$$

for all $t > 0$.

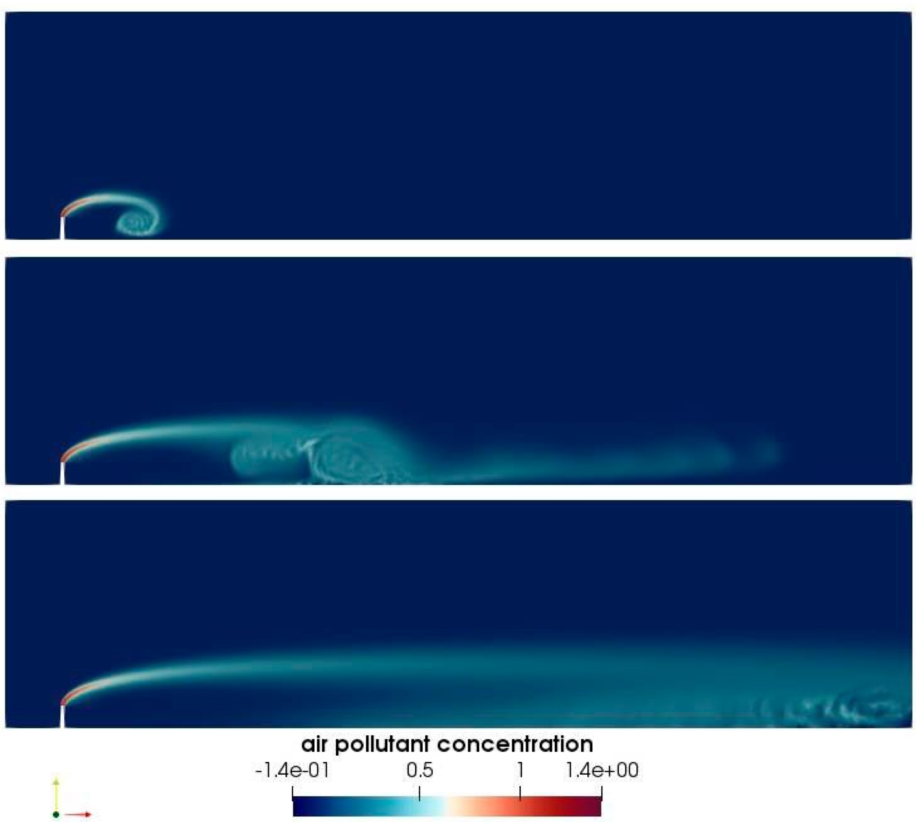

Figure 5. The concentration of the pollutants in the domain Ω emitted steadily with the concentration of $1\ [g/m^2]$ at time 6.72, 44.24, and 165.20 seconds from top to bottom respectively.

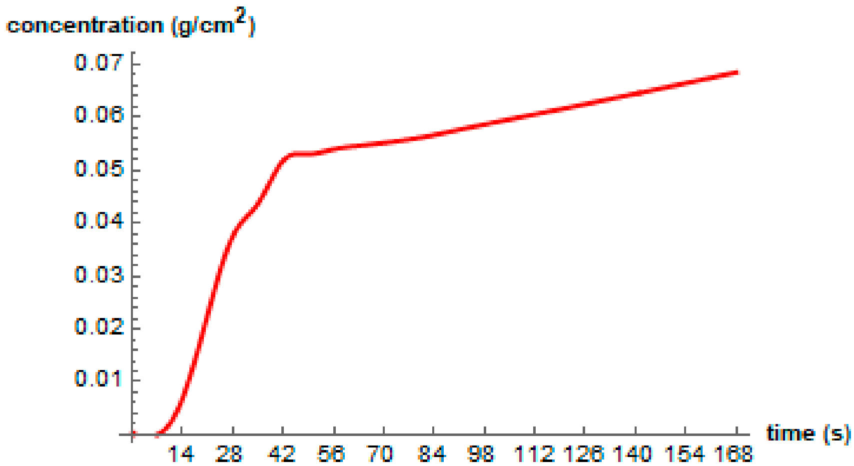

Figure 6. The average concentration of the pollutants steadily emitted with the concentration of $1\ [g/m^2]$ on the observed area Ω_0 as a function of time.

Figure 7 shows the concentration of the air pollutants emitted periodically with the maximum concentration of $1\ [g/m^2]$ and the period of 1.4 seconds at time 6.72, 44.24 and 165.20 seconds. We see that the air pollution propagation is similar to that in Figure 5, where the pollutants are steadily emitted, as the wind velocity and the diffusion coefficient for both cases are identical. However, in contrast to the propagation in Figure 5, the propagation of the pollutants in Figure 7 is more like waves of pollutants. This is not surprising as we assume that the pollutants are generated periodically.

Figure 8 shows the average concentrations of the pollutants which are emitted periodically with the maximum concentrations of $1\ [g/m^2]$ and the period of 1.4 seconds (blue) and the maximum concentration of $2\ [g/m^2]$ and the period of 14 seconds (green) on the observed area Ω_0 as functions of time. It is noticeable that the shape of the average concentration of the case where the pollutants are emitted periodically with the maximum concentrations of $1\ [g/m^2]$ (blue) is very similar to that of the steady emission except that the concentration magnitude is lower.

To compare the average concentration on the observed area between the case of lower maximum concentration but higher emitting frequency (blue) and the higher maximum concentration but lower emitting frequency (green), we see that the observed area is affected by the air pollution quicker for the case with higher maximum concentration despite the lower emitting frequency. However, the average concentration of the case with higher emitting frequency jumps up steeply and is eventually higher than that of the higher maximum concentration. Interestingly, the rates of increase of both cases when the concentrations of the pollutants are rising steeply and in the long run are very similar.

3.3.3 Discontinuous emission

We consider the case where the pollutants are emitted discontinuously with the concentration c_d of $1\ [g/m^2]$ every 1.4 seconds. In other words,

$$C_4(x,t) = \begin{cases} 1, & t = 1.4k \ \text{ for } \ k \in \mathbb{N}_0 \\ 0, & \text{otherwise} \end{cases}$$

for all $t > 0$.

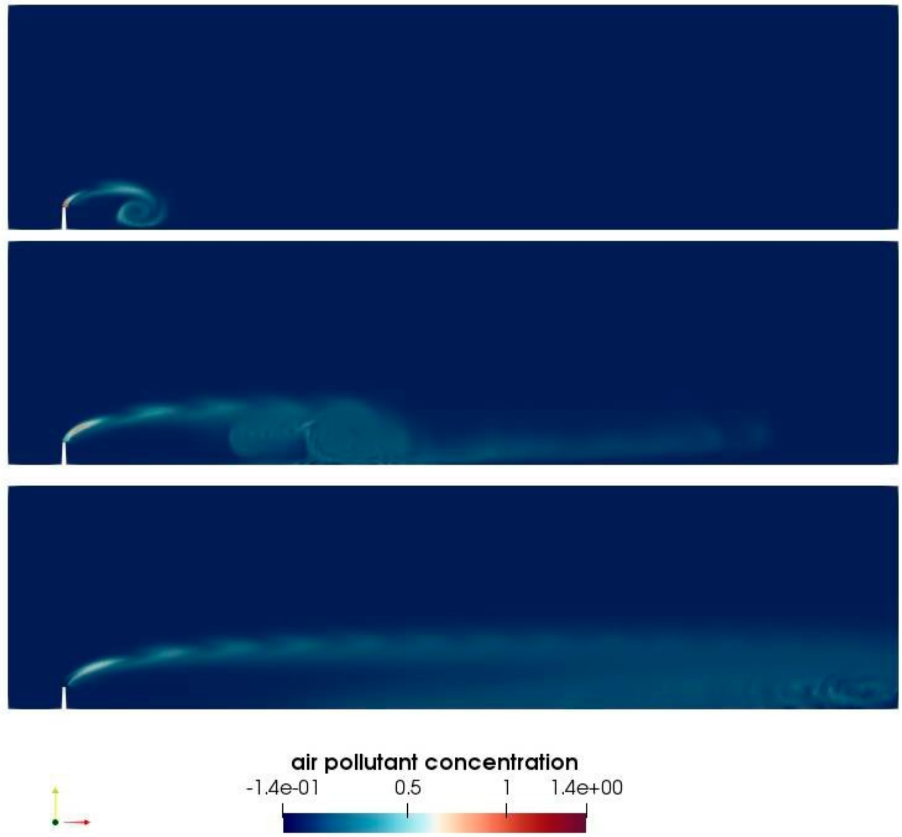

Figure 7. The concentration of the pollutants in the domain Ω emitted periodically with the maximum concentration of $1\ [g/m^2]$ and the period of 1.4 seconds at time 6.72, 44.24, and 165.20 seconds from top to bottom respectively.

Figure 9 shows the propagation of the pollutants in the domain Ω emitted discontinuously with the concentration of $1\ [g/m^2]$ every 1.4 seconds at time 6.72, 44.24, and 165.20 seconds. The propagation is similar to Figures 5 and 7 except that it looks more like chunks of pollutants flowing toward the observed area in the wind direction. This is not surprising as the pollutants are emitted discontinuously.

Figure 10 shows the average concentrations of the pollutants discontinuously emitted with the concentration of $1\ [g/m^2]$ every 1.4 seconds (purple) and the concentration of $8\ [g/m^2]$ every 14 seconds (red) on the observed area Ω_0 as functions of time. We see that the shape of the case with the concentration of $1\ [g/m^2]$ (purple) is similar to that of Figure 6 and the $1\ [g/m^2]$ case of Figure 8. The difference is that the magnitude of the average concentration for the discontinuous emission is lower.

The difference between the cases when the pollutants are discontinuously emitted with lower concentration but higher frequency (purple) and with higher concentration but lower frequency (red) is that the observed area is polluted sooner for the former case but as time goes by, the

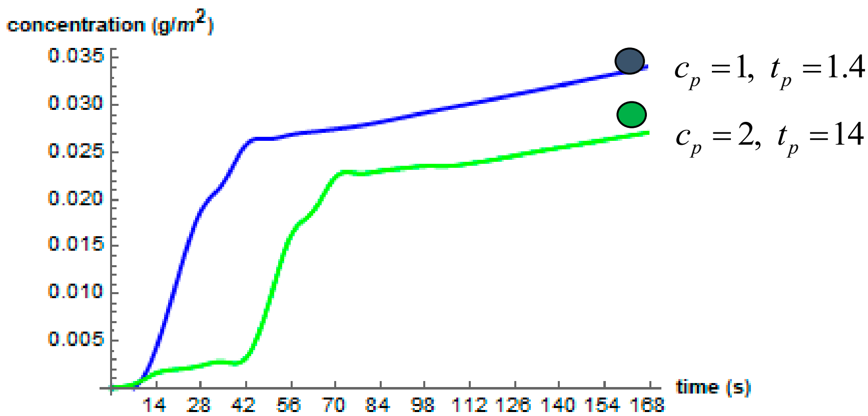

Figure 8. The average concentrations of the pollutants periodically emitted with the maximum concentrations of $1\ [g/m^2]$ and the period of 1.4 seconds (blue) and the maximum concentration of 2 $[g/m^2]$ and the periods of 14 seconds (green) on the observed area Ω_0 as functions of time.

average concentration of the latter case overtakes the former. Eventually, the emission with lower frequency but higher concentration has the steeper rate of increase on the period which it is rising dramatically compared with that of the higher frequency but lower concentration. However, in the long run, the rate of change of the latter is higher than the former.

3.3 Comparison between the Cases

To determine how a given amount of pollutants should be emitted in practice for air pollution management purposes, the comparison between the cases must be made. Given the total amount of the pollutants, $\tilde{C}$, needed to be released from a factory and the total emission time, T, in this subsection, we determine the parameters c_s, c_p and c_d for the steady, periodic, and discontinuous emissions respectively which result in the release of $\tilde{C}$ over the time horizon $[0,T]$.

3.3.1 Steady emission

For the steady emission case, as the total pollutants emitted over $[0,T]$ is $\tilde{C}$, we have that

$$\tilde{C} = \int_0^T c_s dt = c_s T.$$

Thus, the parameter c_s is $\tilde{C}/T$.

3.3.2 Periodic emission

Similar to that of the steady emission case, the total amount of pollutants emitted over $[0,T]$ is

$$\tilde{C} = \int_0^T \frac{c_p}{2}(1-\cos(\frac{\pi t}{t_p}))dt = \frac{c_p}{2}(T - \frac{t_p}{\pi}\sin(\frac{\pi T}{t_p})).$$

To periodically release the total pollutants of $\tilde{C}$ over $[0,T]$, the parameter c_p is $2\tilde{C}/[T-(t_p/\pi)\sin(\pi T/t_p)]$.

3.3.3 Discontinuous emission

For the discontinuous emission case, we have that

$$\tilde{C} = \left\lfloor \frac{T}{t_d} \right\rfloor c_d,$$

where $\lfloor x \rfloor$ is the biggest integer smaller or equal to x. Hence, the parameter c_d is $\tilde{C}/\lfloor T/t_d \rfloor$.

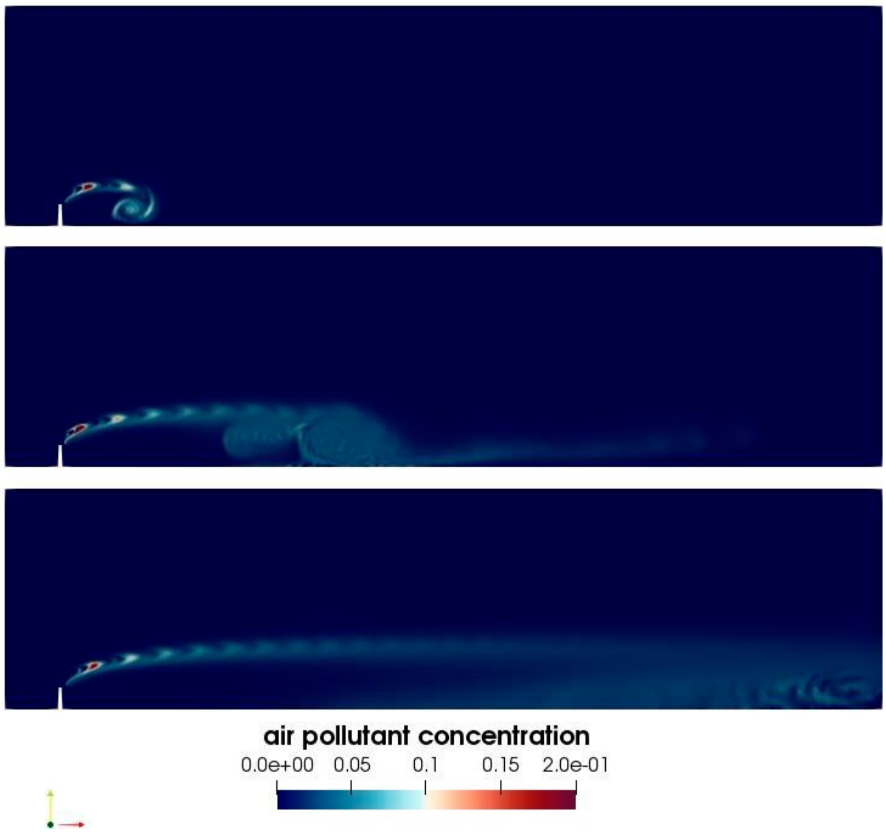

Figure 9. The concentration of the pollutants in the domain Ω emitted discontinuously with the concentration of $1\ [g/m^2]$ every 1.4 seconds at time 6.72, 44.24, and 165.20 seconds from top to bottom respectively.

4. Conclusions

This paper applies the Navier-Stokes and advection-diffusion equations to model the propagation of the pollutants from a single generator such as a tall industrial chimney on an observed area such as a residential area or an agricultural land. We applied the finite element method to numerically solve the model for several cases depending on how the pollutants are emitted over time. The cases are "steady emission", "periodic emission" and "discontinuous emission. We also visualize the propagation of the pollutants from the generator to the observed area over time. In addition, the average concentration of the pollutants on the observed area for each case is also plotted as a function of time.

The visualizations of the air pollution propagation are similar for all cases. We see that the pollutants are blown to the right-hand side of the domain into the observed area and fall to the ground due to the wind and the air pressure. The air circulations can also be observed. The differences are the speeds of the propagations, the concentrations of the pollutants, and the patterns. The emitting pattern of the discontinuous emission case is more like chucks of pollutants rather than a stream. The average concentrations of the pollutants over the observed also area have

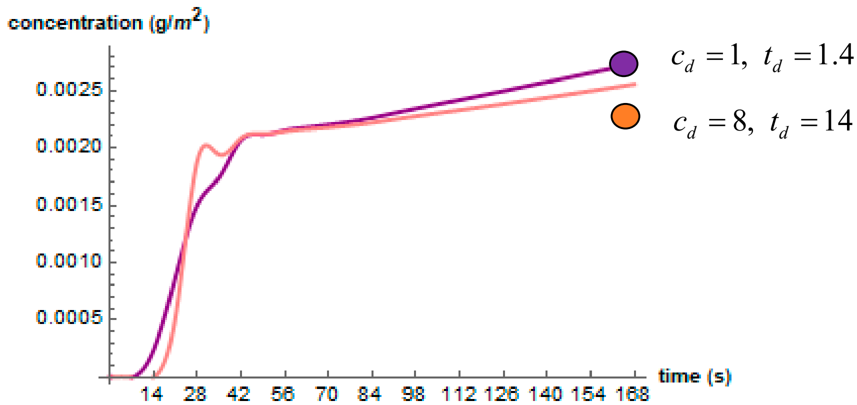

Figure 10. The average concentrations of the pollutants discontinuously emitted with the concentrations of $1\ [g/m^2]$ every 1.4 seconds (purple) and the concentration of 8 $[g/m^2]$ every 14 seconds (red) on the observed area Ω_0 as functions of time.

similar pattern. They start with low concentrations, and at some point, they increase drastically, and eventually increase at constant rates. It is worth noting that if the pollutants are still being emitted, the negative effects from which the observed area is suffering will also be constantly increasing.

This work can be applied to air pollution management problems in order to estimate the concentration of the air pollutants over time on flat domains without obstacles on an observed area such as a residential area. In addition, this can be used to alert people in the observed area if the pollutant concentration is estimated to exceed the fetal level.

Acknowledgements

The authors would like to thank the Development and Promotion of Science and Technology Talents Project (DPST) scholarship as well as Walailak University under the Grant WU64219 for the financial support. We would also like to thank the editor and the reviewers for their thoughtful and constructive comments and efforts towards improving our manuscript. Any remaining errors are the sole responsibility of the authors.

Conflict of Interest Statement

The authors confirm that there is no conflict of interest.

References

[1] World Health Organization., 7 million premature deaths annually linked to air pollution; Available at: https://www.who.int/mediacentre/news/releases/2014/air-pollution/en/.

[2] Unsworth M.H. and Ormrod D.P., *Effects of Gaseous Air Pollution in Agriculture and Horticulture*, Butterworths, London, 1982.

[3] Bell N. and Treshow M., *Air Pollution and Plant Life*, Wiley, Chichester, 2003.

[4] Burney J. and Ramanathan V., *Proc. Natl. Acad. Sci. USA,* 2014; **46**: 16319-16324. DOI 10.1073/pnas.1317275111.

[5] Ghani M., Gueraoui K. and Men-La-Yakhaf

S., *Congrès de Mécanique, Meknès*, Morocco, 11-13 April 2017.

[6] Reddy J.N., *Introduction to the Finite Element Method*, McGraw-Hill Education, New York, 2019.

[7] Olaiju O.A., Hoe Y.S. and Ogunbode E., *Chem. Eng. Trans.*, 2018; **63**: 679-684. DOI 10.3303/CET1863114.

[8] Konglok S.A. and Tangmanee S., *Proceeding in the 3rd National Symposium on Graduate Research*, Nakonratchasrima, Thailand, 18-19 July 2002.

[9] Ulfah S. and Awalludin SA., *J. Phys. Conf. Ser.,* 2018; **948**: 12067-12075. DOI 10.1088/1742-6596/948/1/012067.

[10] Pochai N., *Int. J. Math. Comput. Sci.,* 2011; **5**: 1968-1972. DOI 10.5281/zenodo.1075838.

[11] Oyjinda P. and Pochai N., *Int. J. Diff. Equat.,* 2019; **12**: 1-10. DOI 10.1155/2019/2319831.

[12] Chomcheon S., Khajohnsaksumeth N., Wiwatanapataphee B. and Ge X., *Adv. Differ. Equ-ny.*, 2019; **1**: 459. DOI 10.1186/s13662-019-2382-z.

[13] Zhang Z., Xu X., Qiap L., Gong D., Kim S., Wang Y. and Mao R., *Sci. Rep.*, 2018; **5504**. DOI 10.1038/s41598-018-23880-8.

[14] Temam R., *The Navier-Stokes Equations: Theory and Numerical Analysis*, American Mathematical Society Chelsea Publishing, 2001.

[15] Girault V. and Raviart P.A., *Finite Element Approximation of the Navier-Stokes Equations*, Springer-Verlag, Berlin, 2008.

[16] Hasbani Y., Livne E. and Bercovier M., *Comput. Fluids*, 1983; **11(2)**: 71-83. DOI 10.1016/0045-7930(83)90002-6.

[17] Braack M., *Boundary and Interior Layers, Computational and Asymptotic Methods - BAIL 2014*, Springer, Berlin, 2015.

[18] Geuzaine C. and Remacle J.F., *Int. J. Numer. Meth. Eng.*, 2009; **79(11)**: 1309-1331. DOI 10.1002/nme.2579

[19] Sander O., *DUNE-The Distributed and Unified Numerics Environment*, Springer, Berlin, 2020.

[20] Bastian P., Droske M., Engwer C., Klöfkorn R., Neubauer T., Ohlberger M. and Rumpf M., *Proceedings of the 15th International Conference on Domain Decomposition Methods*, Berlin, Germany, 21-25 July 2003; 167-174.

[21] Kundu P. and Cohen I., *Fluid Mechanics*, Academic Press, London, 2001.

[22] Cannon J.R., *The One-Dimensional Heat Equation*, Cambridge University Press, Cambridge, 2008.